

# A probe for measuring magnetic field profiles inside superconductors from 4.2 K to $T_C$ in high magnetic fields

H D Ramsbottom and D P Hampshire

Superconductivity Group, Department of Physics, University of Durham, Durham, UK

Received 14 March 1995, in final form 5 May 1995, accepted for publication 8 June 1995

**Abstract.** A probe has been designed and built for measuring the magnetization critical current density  $J_C(B, T)$  and magnetic field profiles inside superconducting samples as a function of temperature in large DC magnetic fields. Magnetic field profiles provide a unique opportunity to study the spatial variation of  $J_C$  within a superconducting sample. In these measurements, a small AC field is superimposed upon a much larger DC field. This is the first flux penetration probe capable of making measurements as a function of temperature, in the range 2–30 K (accurate to 100 mK), which combines high AC fields of up to 100 mT (at 19.7 Hz) with very large DC fields of up to 17 T. The probe can be used to study short sections of superconducting cables, wires, tapes, thin films or bulk samples. Its capabilities are demonstrated by presenting variable-temperature data obtained from a commercial multifilamentary NbTi wire in magnetic fields up to 10 T.

## 1. Introduction

Recent developments in cryocooler technology have created the possibility of superconducting applications such as high-field magnets, power cables and SMES [1] operating in a cryogen-free environment at temperatures from 4.2 to 30 K [2]. Variable-temperature analysis is becoming increasingly important in the development of new materials for these applications. In this paper, a new probe is described that can measure the magnetic field profiles of superconductors as a function of magnetic field and temperature. These profiles can be used to determine both the functional form and the spatial variation of  $J_C$ . This provides crucial information for identifying the mechanisms limiting the critical current density.

The next section of the paper highlights the essential principles of flux penetration measurements. Then the design, construction and use of the flux penetration probe are described in detail. This includes a discussion of the external circuitry, coil sets and thermometry. Results are presented on a sample of commercial multifilamentary NbTi wire from 4.2 K to  $T_C$  in DC fields up to 10 T. The data are used to calculate the critical current density and magnetic field profile of the sample as a function of field and temperature.

## 2. Physical principles

Figure 1(a) shows the magnetic field and current profiles inside a cylindrical superconducting sample after applying

a DC field ( $\mu_0 H$ ). In agreement with Lenz's law, lossless supercurrents flow to a depth  $\delta$  to expel the field. Bean's critical state model assumes that, to a first approximation, the maximum current density that can flow is equal to the critical current density ( $J_C$ ). The applied field can be increased until the superconductor is fully penetrated, that is, the depth to which the field penetrates ( $\delta$ ) is equal to the sample radius ( $r_m$ ). At this point, a current density equal to  $J_C$  flows throughout the entire sample.

Flux penetration measurements are made by superimposing an AC field ( $\mu_0 h$ ) onto a large DC field ( $\mu_0 H$ ), as shown in figure 1(b). The shading shows the region of flux motion. The technique involves using a primary coil to generate an AC field and a set of oppositely wound secondary coils to measure the magnetization of the sample. If the two secondary coils, 1 and 2, are of similar geometry but wound in opposite senses and the sample is placed in coil 1, then the voltage across the secondary coils ( $V$ ) can be related to the rate of change of flux ( $d\phi/dt$ ) by

$$V = -k_1 \frac{d}{dt} \left( \mu_0 \int^1 (H + h + M) dS - \mu_0 \int^2 (H + h) dS \right) \quad (1)$$

where  $S$  is a surface integral and  $M$  is the induced magnetization of the sample,  $k_1$  is a constant determined by the coil geometry.

The theory relating the magnetic moment induced in a superconductor to the current density flowing was first outlined by Bean [3]. The critical state model assumes that the current density flowing must be equal either to the critical current density ( $J_C$ ) or to zero. Using this

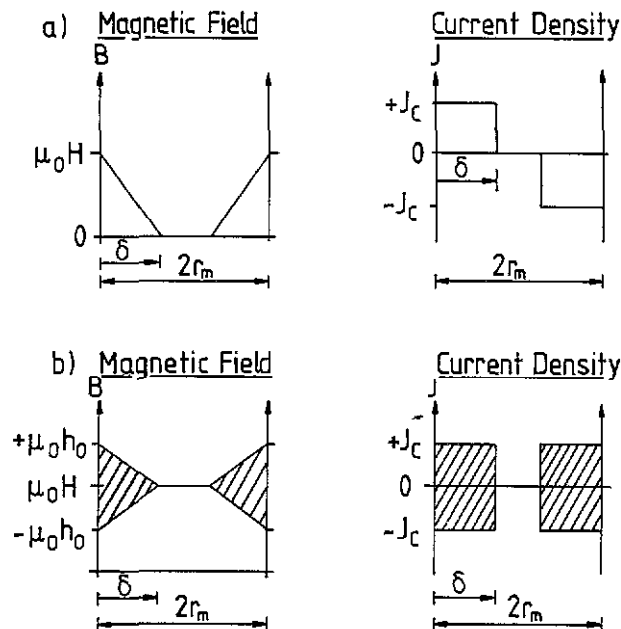


**Figure 1.** The field and current profiles of a superconductor when subjected to a DC field ( $\mu_0 H$ ) and an AC field ( $\mu_0 h$ ), where  $\delta$  is the depth to which the field penetrates and  $r_m$  is the radius of the sample.

model, Campbell considered the magnetic response of a superconductor to an AC field superimposed on a DC field and demonstrated that it can be used to measure the magnetic field profile within the sample [4]. In particular, from equation (1) it can be shown that the minimum voltage across the secondary coils ( $V_M$ ) can be related to the critical current density ( $J_C$ ) by

$$V_M = k_1 k_2 J_C \tag{2}$$

where  $k_1$  is a constant determined by the coil geometry and  $k_2$  is a constant determined by the dimensions of the superconductor.

Equally so for small AC fields, it can be shown that the depth to which the field penetrates ( $\delta$ ) is proportional to the differential of the voltage across the secondary coils with respect to the current through the primary coils ( $dV/dI$ ):

$$\delta = k_3 r_m \left( 1 - \frac{|dV/dI|}{|dV/dI|_{MAX}} \right) \tag{3}$$

where  $r_m$  is the radius of the sample,  $|dV/dI|_{MAX}$  is the maximum value of  $|dV/dI|$  and  $k_3$  is a constant (of the order of unity) determined by the sample geometry. Using Maxwell's equations, the spatial variation of  $J_C$  is given by

$$J_C(\delta) = \left| \frac{dM(\delta)}{d\delta} \right| \tag{4}$$

### 3. System description

#### 3.1. External circuitry

Figure 2 shows the measurement and control system for the flux penetration probe. The AC field is generated using a lock-in amplifier, LIA (Stanford Research Systems), which produces a sine wave output at 19.7 Hz. This voltage is

used to program an 8 A–50 V bipolar operational power supply, BOP (Kepco), which provides the current for the primary coils ( $P_+$ ,  $P_-$  and  $P_{ex}$ ). The current is recorded using a digital multimeter, DMM (Keithley), to measure the voltage across a  $0.01 \Omega$  standard resistor ( $R$ ). The variable DC magnetic field is produced by a 40 mm bore 15/17 T (4.2/2.2 K) superconducting magnet (Oxford Instruments).

The magnetic response of the sample is recorded by using the LIA to measure the voltage induced across a set of oppositely wound secondary coils ( $S_+$  and  $S_-$ ), which are located inside the primary coils. These are configured such that, with no sample present, the total voltage induced across them is approximately zero. A set of external coils ( $P_{ex}$  and  $S_{ex}$ ) are used as a variable inductor to remove any additional out-of-balance signal that can occur when cooling the probe from room temperature to 4.2 K. (The specifications of the coil sets appear later.)

A temperature controller (Lakeshore) is used to control and record the temperature of the sample space ( $T$ ) using a carbon-glass resistance (CGR) thermometer. The atmosphere is maintained at 20 Torr of helium gas using an active pressure controller (MKS), not shown. All external wiring for the thermometry and coil sets consists of co-axial cable and/or screened twisted pairs to reduce noise.

The measurement is computer-controlled using interactive real-time graphical software (ASYST) such that all data are stored digitally. Communication is by IEEE interface except for the magnet power supply that uses the RS-232 bus.

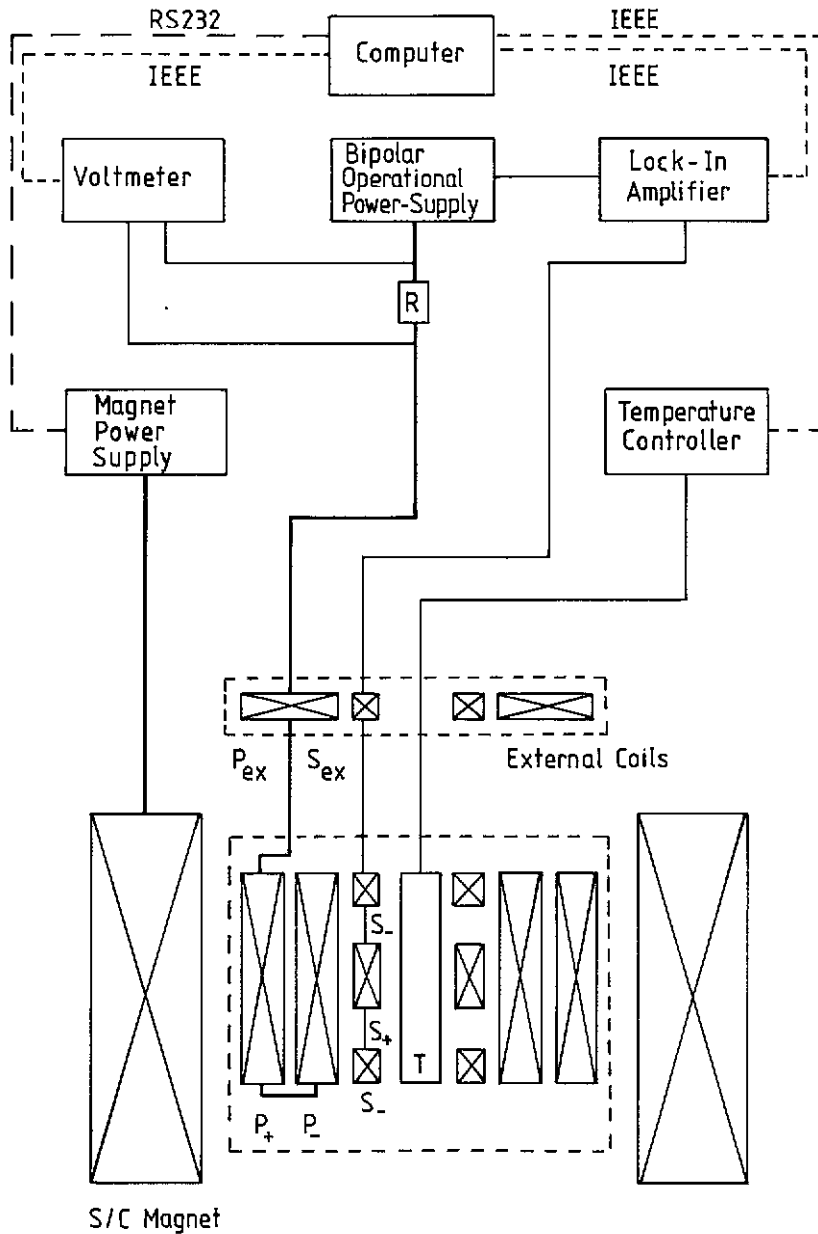
#### 3.2. The top end of probe

Figure 3 shows the top end of the probe. The probe consists of an outer tube (thin-walled stainless steel). Inside this is a vacuum tube (Tufnol). The current leads from the primary coils and the signal leads from the secondary coils lie between these two tubes and travel to the top of the probe where they connect to ten-pin connectors via a clamp (brass). This clamp serves to seal the outer tube and to hold the vacuum tube in place. The vacuum tube extends beyond the clamp to the head of the probe where it makes a fitting with an o-ring seal. During measurements, the probe is mechanically clamped to the top plate of the DC magnet to secure the sample in the field centre and to reduce probe vibrations.

Inside the vacuum tube is an inner tube (stainless steel) which is the pumping line. It does not extend as far as the coil sets. Between the inner tube and vacuum tube is a clearance of 1 mm. It is possible to evacuate this tube through the vacuum valve using a rotary pump. The sample holder (Tufnol) is attached to the inner tube. The thermometry and heater leads travel up the inner tube to two ten-pin connectors at the head of the probe. The total length of the probe is 1.9 m.

#### 3.3. The bottom end of the probe

**3.3.1. The coil sets.** Figure 4 shows the bottom end of the probe. It consists of a set of primary and secondary coils suspended on an outer tube (stainless steel). The



**Figure 2.** The measurement and control system for the flux penetration probe:  $P_+$ ,  $P_-$  and  $P_{ex}$ , primary coils;  $S_+$ ,  $S_-$  and  $S_{ex}$ , secondary coils; and T, constant temperature environment for the superconductor.

primary coil has been limited to a maximum diameter of 38 mm so that it will fit into the bore of the superconducting magnet. The primary coil consists of two, co-axial, oppositely wound coils to reduce the coupling between the coil producing the AC field and the DC magnet [4].

After it had been wound, the two-component primary coil was inserted into the bore of the superconducting DC magnet and the coupling measured by passing an AC current through the primary coil and measuring the voltage induced in the superconducting DC magnet. Turns were added or removed from the outer layer of the primary coil to reduce this induced voltage. When the number of turns on each coil has been optimized and the coils are configured in the opposite sense, the coupling is ten times less than when the coils are configured in the same sense. Reducing the coupling is essential to reduce the vibration of the probe while making measurements in large AC fields.

It is possible to swap between one of two primary coil sets. One consists of a two-component superconducting coil made from 0.3 mm diameter, low-loss multifilamentary NbTi wire (920 304 filaments of 136 nm diameter). Each coil has been impregnated with Apiezon N grease to prevent wire movement from causing the coil to quench prematurely. The maximum field the coil set can produce falls from 100 mT in zero DC field to 0 mT at 10 T, which is the upper critical field of the superconducting wire. However, at DC fields above 7 T, probe vibrations limit the maximum AC field at which data can be obtained to 50 mT at 8 T and 10 mT at 9 T. When measurements at 10 T and above are required, a two-component copper coil is used. This is able to produce an AC field of 10 mT from 0 T to 17 T. The field is limited to 10 mT by the maximum current that can flow before the wire insulation begins to break down. The AC fields produced by the probe are typically

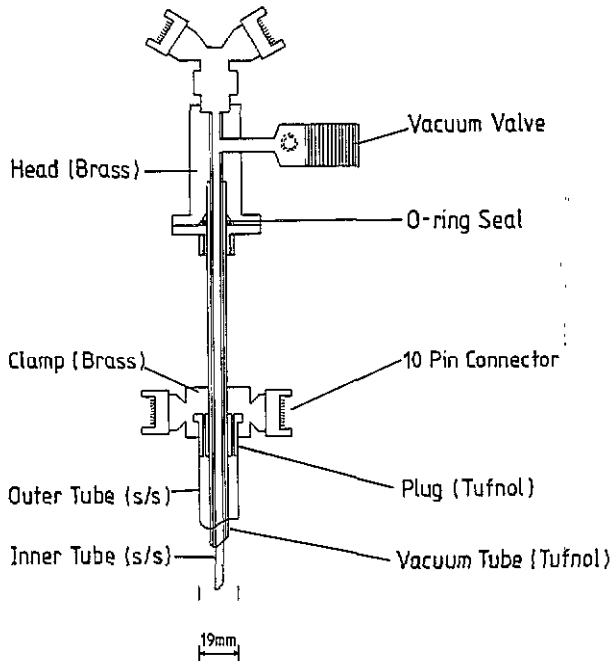


Figure 3. The top end of the flux penetration probe. (Drawn to scale.)

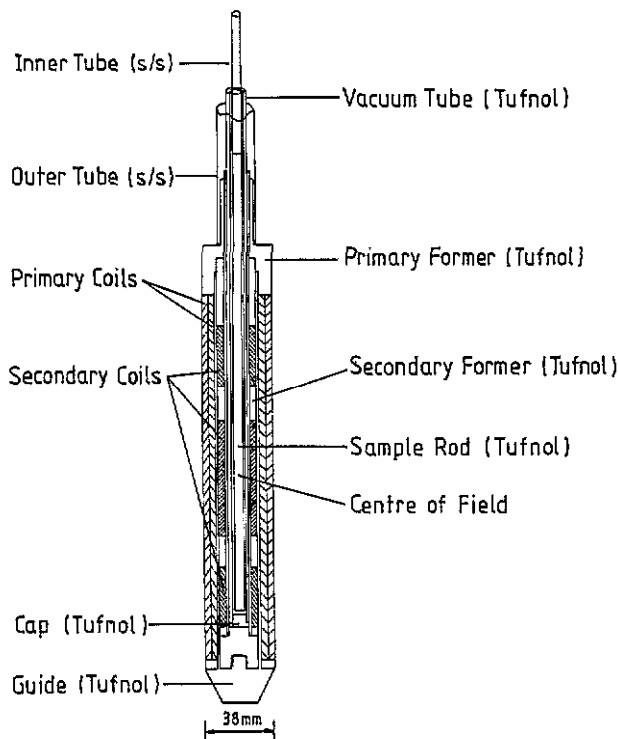


Figure 4. The bottom end of the flux penetration probe. (Drawn to scale.)

a factor of five greater than those of other purpose-built systems and more than a factor of ten larger than those of comparable commercial systems [5].

The superconductor sits in one of the secondary coils ( $S_+$ ) which are co-axial with the primary coils. The other secondary ( $S_-$ ) coil has been separated so that the sample is at the centre of both the AC and DC fields. The secondary coils ( $S_+$  and  $S_-$ ) are configured such that, without a sample present, the total induced voltage across them is zero. The

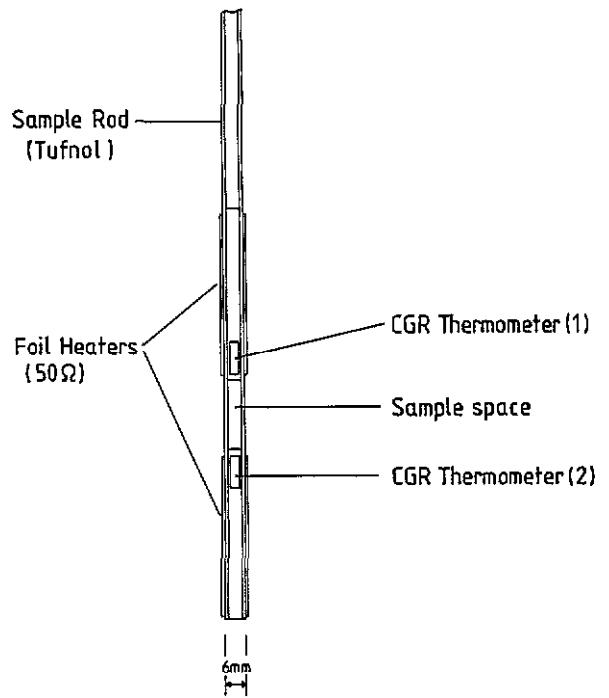


Figure 5. The sample holder and thermometry. (Drawn to scale.)

primary and secondary coils are both wound on Tufnol formers in order to reduce the background signal.

The external coils are at room temperature. These consist of a primary coil ( $P_{ex}$ ) in series with the two-component primary coil ( $P_+$  and  $P_-$ ) and a secondary coil ( $S_{ex}$ ) in series with the  $S_+$  and  $S_-$  coils. The external primary coil is wound using 3 mm diameter wire. (Smaller diameter wire leads to irreproducible results caused by thermal expansion from  $I^2R$  heating at high currents.) The external secondary coil has as few turns as possible (to reduce noise). Table 1 shows a summary of the coil sets used in the probe.

**3.3.2. Thermometry.** Figure 5 shows the sample rod and thermometry. The sample sits between two commercially calibrated CGR thermometers. These have small and reproducible magnetic-field-induced changes in resistance [6]. Both thermometers have previously been calibrated in our laboratory as a function of magnetic field up to 15 T. One of the thermometers is read by the temperature controller and used to record and control the temperature. The second thermometer is used to measure temperature gradients across the sample. (Its resistance is recorded using a constant current source (Lakeshore) and DMM (Keithley), not shown in figure 2.) Two cylindrically wrapped foil heaters ( $50 \Omega$ ) are used to control the temperature. These are wired in parallel so that a potentiometer can be used to vary the ratio of power to each heater. In this way it is possible to minimize the temperature gradients across the sample.

The sample, thermometers and heaters are all mounted on a Tufnol rod and surrounded by vacuum grease. This is contained in a Tufnol tube within which the atmosphere is controlled to be 20 Torr of helium gas. By using these

**Table 1.** A summary of coil dimensions.

Coil set	Material	Wire diameter (mm)	Coil length (mm)	Inner diameter (mm)	Outer diameter (mm)	Number of turns
P <sub>ex</sub>	Cu	3.00	100	20	100	500
P <sub>+</sub>	Cu	0.25	215	20	30	1800
P <sub>-</sub>	Cu	0.25	215	30	38	1400
P <sub>+</sub>	NbTi	0.30	215	20	30	12500
P <sub>-</sub>	NbTi	0.30	215	30	38	10000
S <sub>ex</sub>	Cu	0.25	80	10	12	1250
S <sub>+</sub>	Cu	0.25	68	12	18	3500
S <sub>-</sub>	Cu	0.25	34	12	18	1750

techniques, it is possible to achieve a sample temperature accuracy of better than 100 mK from 4.2 K to 30 K in magnetic fields up to 15 T.

### 3.4. General design considerations

When high AC currents flow in the primary coil, Joule heating produces cold helium gas. Some of this gas flows past the current leads via several holes in the outer tube. This gas prevents the current leads from overheating and reduces helium consumption. The thermal connections from room temperature to the liquid helium bath are primarily via Tufnol or thin-walled stainless steel tubing. These choices of material also reduce helium consumption while maintaining sufficient mechanical strength.

### 4. System operation

Initially, the sample space is evacuated using a rotary pump and flushed with helium gas. This process is repeated three times. The DC field is set to the required value and the maximum AC field supplied by the primary coil. The superconductor is then heated into the normal state and the external coils used to set the net voltage across all of the secondary coils to zero. When properly balanced, the voltage across the secondary coils is less than  $10^5$  times that across just one of them. The LIA is phased using the voltage across a  $0.01 \Omega$  standard resistor in series with the primary coils. This enables measurements to be made both in-phase (lossless) and out-of-phase (with loss) with respect to the AC field. The AC field is then set to zero.

The first temperature is set using the temperature controller and any temperature gradient across the sample minimized. When the temperature has stabilized at the required value, the primary current is ramped at  $0.05 \text{ A s}^{-1}$  (that is, the AC field is increased) and recorded using the standard resistor and DMM. The in-phase voltage produced across the secondary coils is simultaneously recorded using the LIA. A frequency of 19.7 Hz is used because it is a compromise between approaching the DC limit and achieving a good signal-to-noise ratio. The AC field is then set to zero. This is repeated for each temperature at this DC field. After measurements have been completed for all temperatures required, the magnetic field is changed, the secondary coils re-balanced and the measurement procedure repeated. In this way a complete set of data is obtained at all temperatures and magnetic fields.

In the procedure outlined above, the secondary coils are balanced at each DC field and subsequent measurements made as a function of temperature. This is preferable to holding the temperature fixed and making measurements as a function of magnetic field because the background signal has a large dependence on the DC field, approximately  $0.2 \text{ mV A}^{-1} \text{ T}^{-1}$ . This is comparable in size to the signal from the sample. The temperature-dependence of the background signal is almost negligible, approximately  $2 \mu\text{V A}^{-1} \text{ K}^{-1}$ .

### 5. Results and discussion

In this paper the probe's capabilities are demonstrated by presenting data on a commercial NbTi wire. The wire consists of 61 filaments each of diameter  $28 \mu\text{m}$ . The copper matrix was removed using nitric acid and the NbTi filaments stuck together using GE varnish. 60 sections were cut, each 3 mm long and formed into a sample. The sample was positioned in the probe such that the AC field was perpendicular to the axis of the NbTi filaments.

Figure 6 shows the magnetic moment versus AC field as a function of temperature at 3 T. In figure 6 the experimentally measured quantities are included, namely the current through the primary coil and the voltage across the secondary coils. The background signal has been subtracted from all data. At all temperatures there is a sharp fall in the magnetic moment to a minimum value when there is full penetration of the superconductor. After this, the magnetic moment slowly increases as the AC field increases beyond that required for full penetration. The marked increase in magnetic moment at low temperatures and high AC fields (below the broken line) is attributed to eddy current heating in the copper components of the probe. The small oscillations in the traces are due to small oscillations in temperature.

From the minimum value of the magnetic moment, the coil geometry and the dimensions of the sample, it is possible to calculate the magnetization critical current density at each magnetic field and temperature,  $J_c(B, T)$ , see equation (2). Figure 7 shows the  $J_c(B, T)$  plot for the NbTi sample. The uncertainty in the values of  $J_c(B, T)$  is approximately 10%, primarily due to uncertainty in the sample dimensions. The data suggest that  $J_c$  is greater than  $2 \times 10^9 \text{ A m}^{-2}$  at 5 T at 4.2 K, which is in good agreement with the literature value [7].

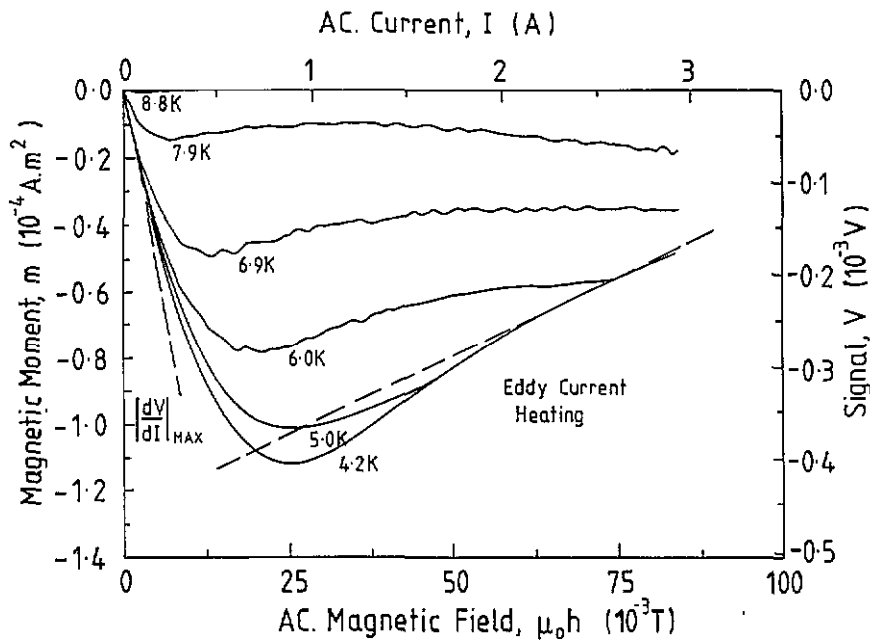


Figure 6. The magnetic moment versus AC field for NbTi as a function of temperature at 3 T. In the region below the broken line, eddy current heating prevents effective temperature control.

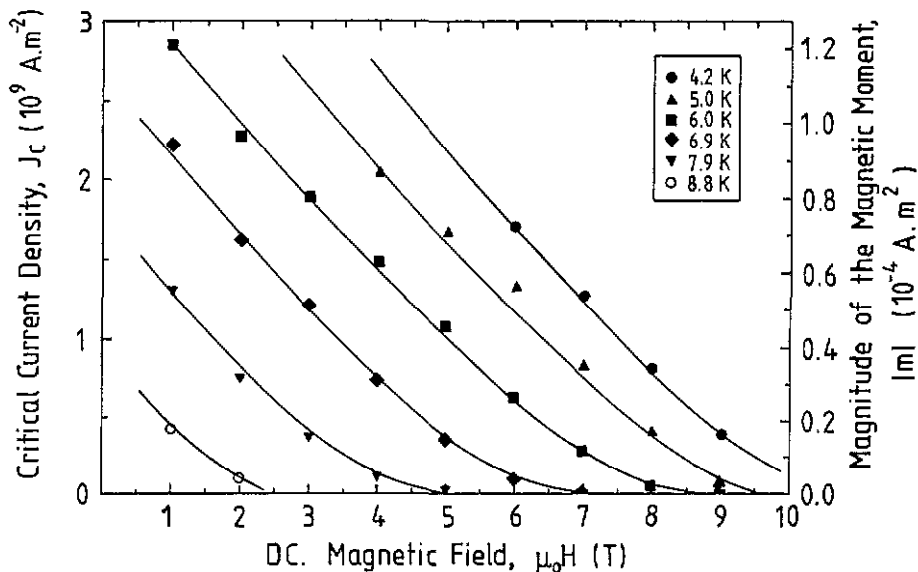
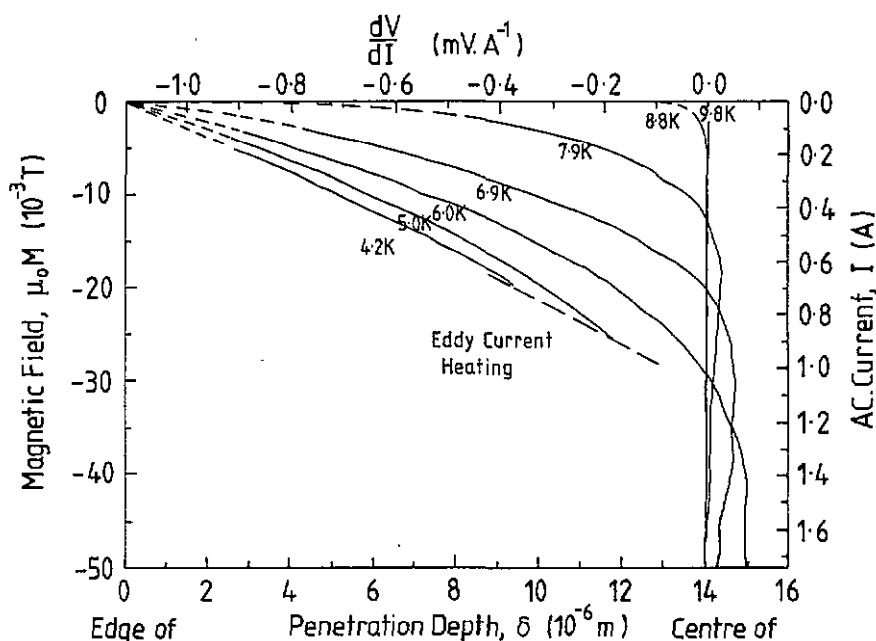


Figure 7. The magnetization critical current density of NbTi as a function of field and temperature.

By following the analysis outlined by Campbell and differentiating the data in figure 6, it is possible to determine the magnetic field profile inside the NbTi sample, see equation (3). Figure 8 shows the spatial variation in the magnetic field ( $\mu_0 M$ ) in the superconductor as a function of temperature at 3 T. The applied DC field  $\mu_0 H$  and AC field  $\mu_0 h$  can be superimposed onto  $\mu_0 M$  to give the net field  $B$ . Figure 8 also shows the region of high AC fields at low temperatures beyond which temperature control cannot be maintained due to eddy current heating. The field appears to penetrate to a distance greater than

the sample radius. The analysis shows that this is an artefact which results from the applied AC field being larger than that required for full penetration [8]. Equation (4) demonstrates that the gradient of the lines as a function of penetration depth gives the spatial dependence of the critical current density. It can be seen that the gradient of the line (and hence  $J_c$ ) is approximately constant throughout the sample. Hence surface pinning is not a significant mechanism in this material. This is expected for a bulk pinning superconductor such as NbTi.



**Figure 8.** The magnetic field profile inside a NbTi sample as a function of temperature in a DC field of 3 T. In the region below the broken line, eddy current heating prevents effective temperature control.

## 6. Conclusion

A probe has been designed for making flux penetration measurements on superconducting samples from 4.2 to 30 K, accurate to 100 mK, in high magnetic fields up to 17 T. The probe can use one of two different coil sets to generate an AC field. One is made from copper wire and can produce an AC field of 10 mT from 0 to 17 T. The other uses a superconducting NbTi coil, which can generate a much larger AC field (up to ten times larger in zero DC field). The capability of the probe has been demonstrated on a commercial multifilamentary NbTi wire. The data have been analysed using Bean's critical state model to calculate the critical current density as a function of field and temperature. The value obtained compares well with the literature. Campbell's analysis has also been used to generate the magnetic field profile inside the superconducting sample. These profiles give the spatial variation of  $J_C$  from which it is possible to distinguish surface pinning from bulk pinning and hence better determine the mechanisms that limit  $J_C$ .

## Acknowledgments

The authors wish to acknowledge G Teasdale and P Collins for the construction of the probe and thank P Russell for help with production of the drawings. This work was

supported by the EPSRC GR/J39588 and the Royal Society, UK.

## References

- [1] Larbalestier D C 1991 Critical currents and magnet applications of high- $T_C$  superconductors *Phys. Today* June 74–82
- [2] Tozai N 1994 Liquid-helium free refrigeration for superconducting magnets *Superconductor Industry* Spring 41–2
- [3] Bean C P 1964 Magnetization of high field superconductors *Rev. Mod. Phys.* **36** 31–9
- [4] Campbell A M 1969 The response of pinned flux vortices to low frequency field *J. Phys. C: Solid State Phys.* **2** 1492–501
- [5] Campbell A M and Blunt F J 1990 Proving self field effects on intergrain currents using an AC technique *Physica C* **172** 253–9
- [6] Sample H H, Brandt B L and Rubin L G 1982 Low-temperature thermometry in high magnetic fields. V Carbon-glass resistors *Rev. Sci. Instrum.* **53** 1129–36
- [7] Friend C M and Hampshire D P 1993 Transverse and longitudinal critical current densities in Nb 46.5% wt Ti multifilamentary wire from 4.2 K up to  $T_C$  in magnetic fields up to 15 T *Applied Superconductivity Vol.1. Proc. European Conf. on Applied Superconductivity (Germany: DGM Informationsgesellschaft mbH)* pp 23–6
- [8] Ramsbottom H D and Hampshire D P 1995 Campbell's analysis used to calculate the flux profiles of NbTi from 4.2 K to  $T_C$  in magnetic fields up to 10 T *J. Phys. C: Solid State Phys.* to be submitted